Hybrid Radio Tomographic Imaging: Potential Localization for Human Detection in Outdoor Environment

M.T.M Talib[1,2], M.H.F Rahiman[1,2*], R.A. Rahim[3], M.S.M. Abdullah [1,2]

[1]Faculty of Electrical Engineering Technology, Universiti Malaysia Perlis, Pauh Putra Campus, 02600 Arau, Perlis, Malaysia
[2*]Center of Excellence for Advanced Sensor Technology (CEASTech), Universiti Malaysia Perlis, 02600 Arau, Perlis, Malaysia
[3]School of Electrical Engineering, Faculty of Engineering, Universiti Teknologi Malaysia, 81310 Skudai, Johor, Malaysia

Corresponding author* email: hafiz@unimap.edu..my
Accepted 3 March 2021, available online 31 March 2021

ABSTRACT

Radio Frequency Tomography (RTI) is a technique use to localize the human position. This approach offers great potential in monitoring activities such as perimeter surveillance monitoring, virtual fence for farm monitoring, and residential monitoring. Conventionally, RTI uses Linear Back Projection algorithm (LBP) to reconstruct the tomographic image. However, the ill-posed problem caused by back-projection and the smearing effect due to the overlapping image produce a low-quality tomographic image. To improve the quality tomographic image, several regularization approaches has been introduced by other researchers. These regularization techniques used in RTI to eliminate the smearing impact on the RTI image. However, because the target occupies only a small amount of space compared to the entire area monitored, the resulting image is blurred with noise. Thus, this paper proposed a Hybrid Radio Tomographic Imaging (HRTI) to overcome this problem. Our main focus is to improve the quality of RTI image by reducing the smeared area. In this approach, threshold sensor value has been introduced to reduce the impact of noise. By applying the HRTI, the average of reconstruction error can be reduced and accuracy localization of HRTI exceed 96%.

Keywords: Radio Tomographic Imaging, Device free localization

1. Introduction

Radio Frequency Tomography (RTI) is a technique use to localize the human position presented by Wilson and Patwari in 2009 [1]. The cross-section image of a monitoring area is constructed by analyzing the receive signal strength (RSS) value and the attenuation of the radio frequency (RF) signal [1]. This approach offers great potential in monitoring activities such as perimeter surveillance monitoring, virtual fence for farm monitoring, and residential monitoring. Conventionally, RTI uses Linear Back Projection algorithm (LBP) to reconstruct the tomographic image. The fundamental of the LBP algorithm is the multiplication of the sensitivity matrix with the appropriate RSS value. Although, RTI gives significant result in localization, however, the ill-posed problem caused by back-projection and the smearing effect due to the overlapping image produce a low-quality tomographic image [2]. This problem leads to low localization accuracy. To improve the quality tomographic image, several regularization approaches has been introduced. Tikhonov regularization truncated singular value decomposition (TSVD), total variation (TV), and compressive sensing (CS) algorithm are three standard regularization techniques used in RTI to eliminate the smearing impact in order to improve the quality of tomographic image and increase the localization accuracy [1][2]. Compares to the total variation (TV), and compressive sensing (CS), Tikhonov regularization truncated singular value decomposition (TSVD) gives an acceptable localization accuracy. However, the resulting image is blurred with noise and interferes with target detection because the target occupies only a small amount of space compared to the entire area monitored [2][3]. Thus, several researchers have given their attention to studying the combination of different regularization techniques to solve the quality image problem. Xu et al. [12] propose a new reconstruction regularization by combining Tikhonov regularization and least absolute shrinkage and selection operator (LASSO) regression method, exploiting both the sparsity and correlation inherent in the attenuation image linearly. In this research, he proposes to

utilize spatial diversity by using multiple antennae. The localization is more robust using this technique because it can record the difference in RF characteristics of each antenna pair. The image quality of this technique is always much higher than that of Tikhonov, and it can locate the target more accurately compare to LASSO regularization. However, the limitation of the method is it requires more nodes to achieve the desired accuracy, which can increase the development cost and make it impractical.

Therefore, this paper introduced a Hybrid Radio Tomographic Imaging (HRTI). In this approach, threshold sensor values (TSV) has been introduced to reduce the impact of noise due to shadowing effect of measurement in the image reconstruction.

2. The Model of Radio Tomographic Imaging

The Radio Tomographic Imaging Model has been developed using a wireless sensors network. The number of sensors nodes (N) has been arranged outside the monitoring area as shown in figure 1. The total number of measurements of wireless sensor network can be obtained by M=N(N-1) by assuming the reciprocal of the measurement link are not equal due to differences in shadowing loss in each link caused by noise. From the observation of RSS attenuation, if there is an object in the monitoring area, the RSS value is around -60dBm to -80dBm. This attenuation of the RF signal is due to object obstruction. The attenuation of radio signal strength (S_{att}) can be obtained by equation 1.

$$S_{att} = M_{int} - M_{att} \quad (1)$$

Where, M_{att} is RSS measurement when object exist in the monitoring area while M_{int} is RSS measurement under initial condition (empty area). To obtain the attenuation images, the wireless network has been modeled as a pixel grid with the size of m x n. To fulfill this, the imaging area is divided into several small square areas which have the same size to represent the pixels. There is no limit in determining the number of pixels uses. However, fewer pixels will result in low-quality pictures while a large number of pixels results in high computational time.

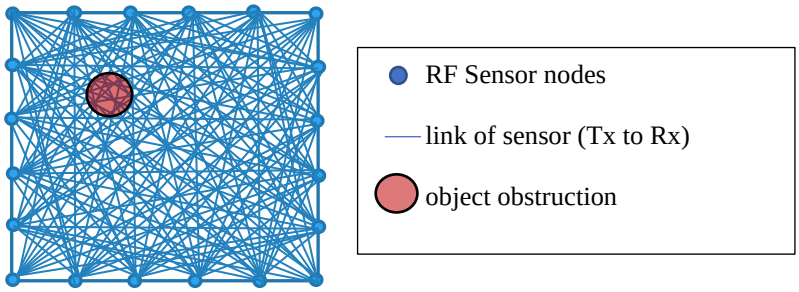

Figure. 1. Model of Radio Tomographic Imaging with wireless sensor network

It is important to know which pixels are intersected by the sensor link line because that information is used to determine the value of the pixels in the reconstructed image. There are many models such as line model and elliptical model to determining which pixels influence a link then will weighting them accordingly. This signal disruption model is to helps in determining how the link signal strength is interrupted by objects in the network.

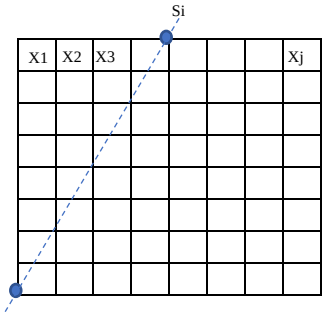

Figure. 2. A RF network link travel on the Line of sight (LOS) path

In Figure 2, x_j is refer to the attenuation when the signal passes through pixels j while S_i can be seen as a weighted sum x_j [1]. From illustration in Figure 2, the attenuation (S) can be modelled as

$$S_i(t) = \sum_{j=1}^{N} \omega_{ij} x_j(t) \tag{2}$$

where $x_j(t)$ is a single link attenuation, and ω_{ij} is the weight for each link. Since the attenuation occurs only on pixels located in the LOS path, then the weight of pixels not located in the LOS path should be zero. Further, a sensitivity map is a sensitivity propagation plot obtained by calculating the radio frequency attenuation at the position of each receiver due to obstructions in the monitoring space. In this paper, we explore the Gaussian Model in determining the link signal strength affected due to the object obstruction.

2.1 Gaussian Model

The Gaussian model is a new signal disruption model has been introduced in this research. It can be used as an alternative method besides the elliptical model. We assume that the propagation of environmental noise including multipath interference is corresponding to a normal or Gaussian distribution [4]. Through this model, the Gaussian function has been applied to provide pixel weights. Referring to general gaussian equation expressed in equation (3) and Figure 3, α is the peak of the curve, μ is center of the peak and σ is the standard deviation that control the peak' width. Through this model, pixel's weight is assign depending on the pixel distance from LOS path as stated in equation (4). Where, d_l is the length of the LOS path between two sensor nodes and $d_{l,p}$ is the total distance from the two sensor nodes to the center of the pixel. If the pixel lies on the LOS path, it will have the highest weight while the pixel farthest from the LOS will get the lowest weight as shown in figure 4.

$$f(x) = \alpha e^{-(\frac{x-\mu)^2}{2\sigma^2}} \tag{3}$$

$$\omega_{l,p} = e^{-(\frac{d_{l,p}-d_l)^2}{2\sigma^2}} \tag{4}$$

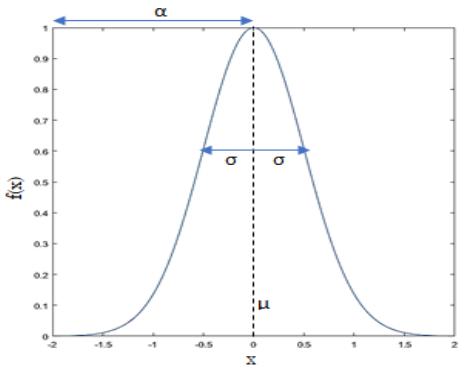

Figure. 3. Gaussian function with α=1, μ=0, σ=0.5

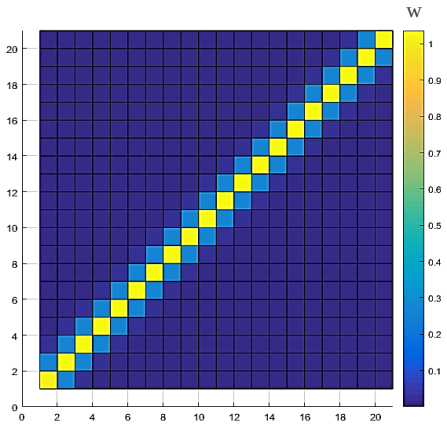

Figure. 4. Gaussian function with α=1, μ=0, σ=0.5

Meanwhile, figure 5 shows a tomographic image of human location projected by Gaussian model. In this RTI image, the red color in this image represent the high permittivity area which contain the information of human location.

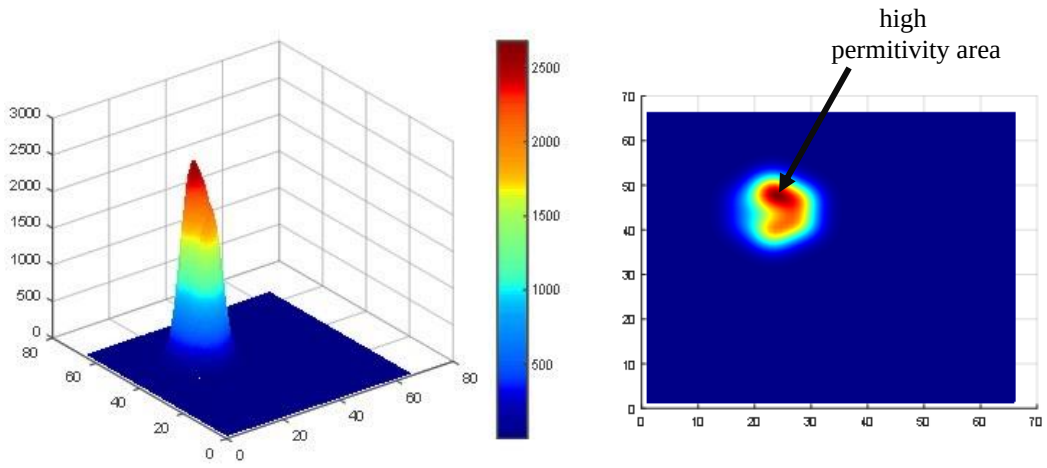

Figure. 5. Tomographic image of human location projected by Gaussian model

2.2 Hybrid Radio Tomographic Imaging approach (HRTI)

Another image reconstruction technique named as Hybrid Radio Tomographic Imaging (HRTI) has been introduced. This approach is obtained by multiplying each sensor value with its sensitivity map same as Linear Back Projection (LBP). However, in this H-RTI approach, if the normalized sensor value $N_{Tx,Rx}$ is more than or equal to threshold value Nr, then its sensitivity map is set to the maximum pixel value (i.e., 255). But, if the normalized sensor value is less than threshold value, it is set to minimum pixel value which is zero.

This threshold value refers to the normal ratio of RF attenuation obstructed by the human body. In this experiment, an adult with a medium size (body circumference about 50 cm) was used as a model. From observation, found that the normalized attenuation ratio is 0.2. However, the threshold value depends on the human size. If the size of the human body is bigger, then the attenuation is higher. Thus, the threshold value will exceed 0.2. This threshold value is needed to filter up the highly effected link data and remove the low effected link data. The mathematical model for H-RTI is stated as follows

$$A_{H-RTI}(i,j) = \sum_{Tx=1}^{20} \sum_{Rx=1}^{20} N_{Tx,Rx} \times \bar{M}_{Tx,Rx}(i,j) \quad (5)$$

$$A_{H-RTI}(i,j) = \begin{cases} 1 & if\ N_{(Tx,Rx)} \geq N_r \\ 0 & if\ N_{(Tx,Rx)} < N_r \end{cases} \quad (6)$$

Where, $\bar{M}_{Tx,Rx}(i,j)$ is a sensitivity map generated based on the gaussian model. From figure 6, it is clearly seen that the smeared area in the RTI image has been reduced using the HRTI approach. By reducing the smeared area on the RTI image, we can minimize the red area in the image. This will indicate the focus of the exact location of the human.

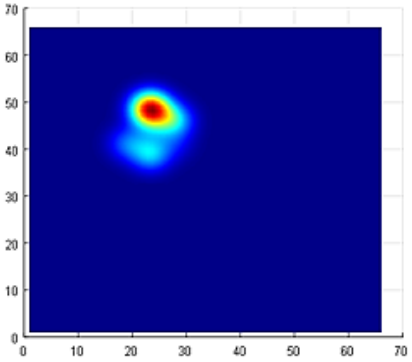

Figure. 6. Tomographic image of human location projected by HRTI

3. Experimental Design

An experiment has been designed to gather information about the human body attenuation. The information about RSS data for both stage (calibration and attenuation) help in designing the system model. By taking the average diameter of the human body is 50cm, monitoring area of 5m x 5m has been divided into nine grids to represent a zone, as shown in figure 7(a). Hence, each zone can contain up to five positions of human. Figure 7(b) shows the affected pair of the link, which gives high attenuated data. Where the area in the circle contains high attenuated data, which presents the human position in the monitoring area. Figure 8 shows the experimental setup for monitoring area of 5m x 5m. The RSS value of the baseline dataset collected under the calibration period (without the presence of human).

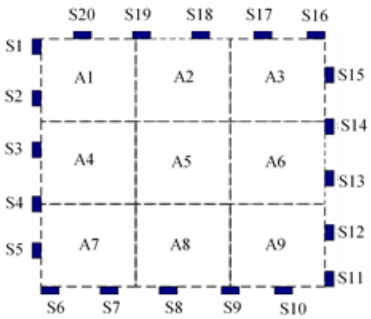

(a) 9 zone of monitoring area

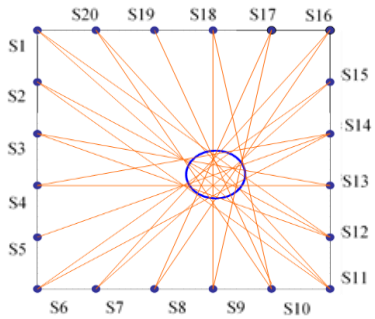

(b) Effected pair of links due to human presence

Figure. 7. Experimental design for human localization

Figure. 8. Sensor array follow experimental design

To perform the measurements, a square monitoring area as shown in figure 7 (a) with dimensions of 5 meters x 5 meters was prepared for the experiment. The monitoring area was arranged with 20 units of RTI sensors with a spacing of one meter each. The experiment was conducted in two conditions; (i) in the empty state and (ii) in the obstructed state with the human. During this measurement period, the human is in rest position at each location mark. These observations were made to observe the effect of the human body on RSSI measurements. Figure 7 (b) shows a single scan transmitter to several reception sensors where the red line in this figure is the affected link due to the presence of humans providing attenuation data. From these experiments, RSS measurements for a single scanning transmitter (TX) to several reception sensors (RX) showed that the RSSI range without human body attenuation was around -40 to -60 dBm, while the human body attenuation was around -61 dBm to -80 dBm. In this experiment, each sensor acts as a transceiver. For example, in a single scan, sensor (S2) sends a signal while another sensor will receive the signal sent by S2. The scanning process will be repeated until all sensors send a signal. The attenuation of radio signal strength due to human presence can be obtained as

$$Att_{(Tx,Rx)} = M_{ref-} M_{(Tx,Rx)} \tag{7}$$

Where $M_{(Tx,Rx)}$ is attenuation data for the current human position, and M_{ref} is reference data during an empty area (baseline). The link measurements are considered to be simultaneous and all the parameters in (7) are arranged in the matrices form.

4. Result and discussion

4.1 Performance analysis of image reconstruction method

Performance analysis was performed on Gaussian and HRTI methods to evaluate the effectiveness of the approach. Table 1 illustrates the comparison of the image projected by Gaussian and HRTI for one location of human. From the result, the quality images generated by the Gaussian are still low due to large smeared areas on the image and introduces a localization in the wrong place. It is hard to obtain a correct location of human with high accuracy due to smeared areas. On the contrary, the quality image reconstructed by HRTI is better compared to the image projected by Gaussian. Through this method, the smeared area on the image has been reduced. This approach was also tested with a situation where there were two humans in the monitoring area as shown in Table 2. Typically, the problem faced by Linear Back Projection and Gaussian is that reconstructed images of two closer human positions tend to merge together. Therefore, the problem of merging 2 nearby human locations can be solved by introducing the HRTI method.

Table 1. Reconstructed image of Gaussian and HRTI approach for one human

PHANTOM	Gaussian	HRTI
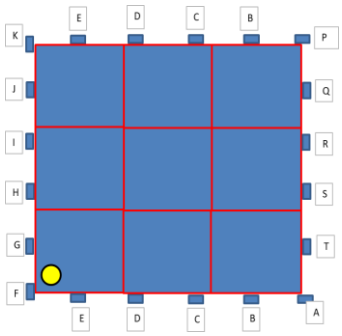 Sample 1	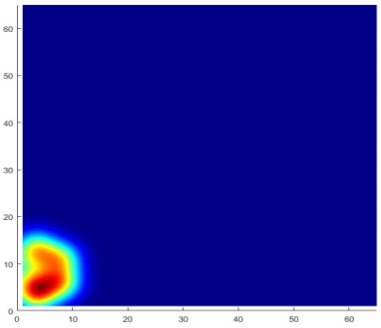	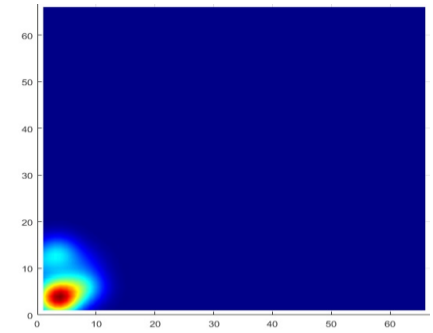
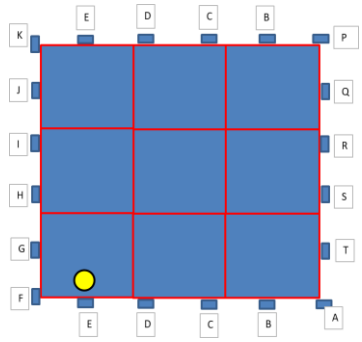 Sample 2	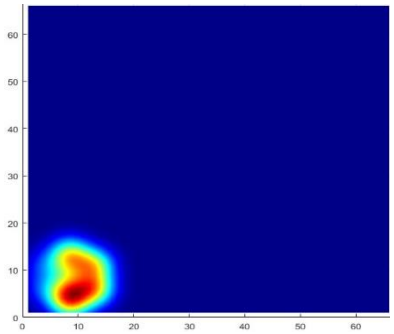	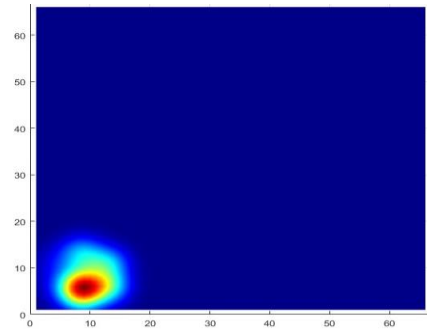
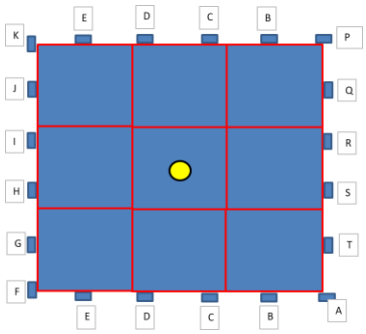 Sample 3	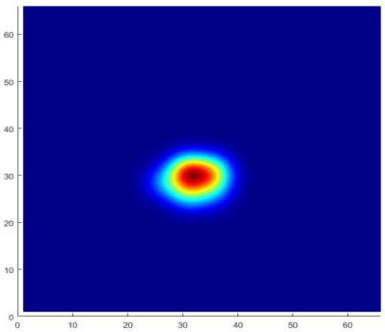	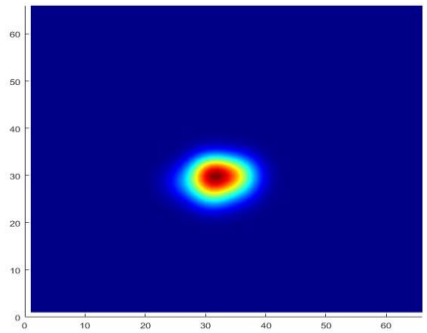

Table 2. Reconstructed image of Gaussian and HRTI approach for two humans

PHANTOM	Gaussian	HRTI
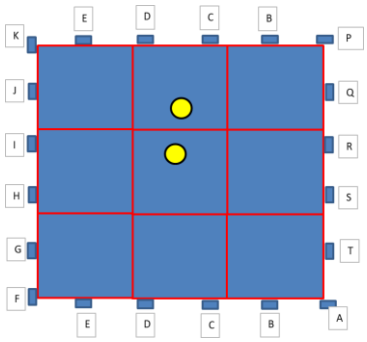	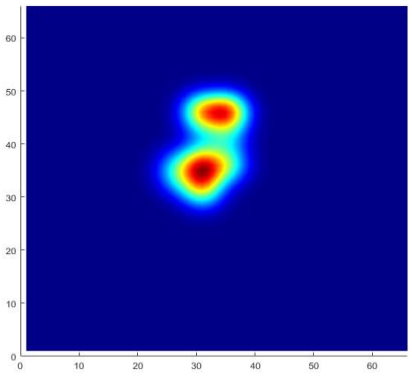	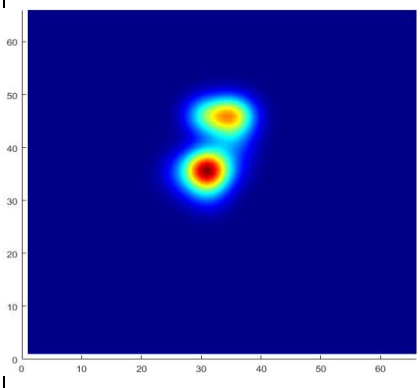
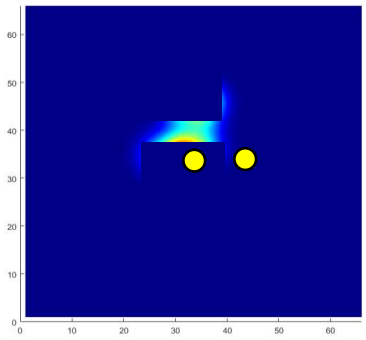	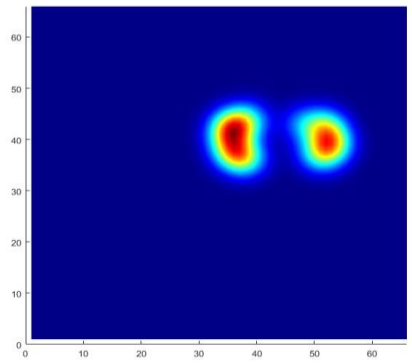	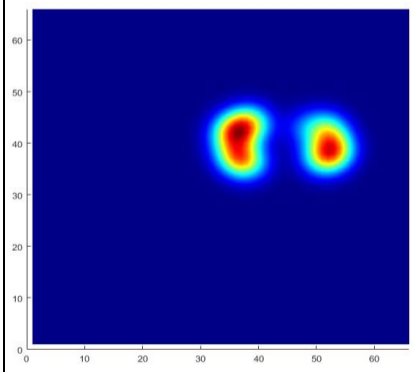

The quality of tomographic imaging can be assessed by comparing image of reconstructed physical models with actual cross-sections [5]. The comparisons are made based on reconstructed image with standard image corresponding to the cross section of the physical model [6][7]. Where, the standard image is an array of M pixels defining the standard (test) model by the color level of each pixel. In this analysis, the area error percentage (AE%) was calculated based on colored pixels which representing the permittivity levels. The summation of colored pixel then will be divided by the total number of pixels of an image. Table 3 illustrates the result of AE% for comparison. The area error percentage of HRTI is lower than 3% while the area error percentage of Gaussian is slightly higher for all tested samples. Thus, known that the performance of HRTI is better compared to Gaussian. the graphical plot in Figure 9 can be referenced for a clear view. Furthermore, accuracy is a main concern to evaluate the effectiveness of the method. Since area errors have been reduced, localization accuracy can be improved. Table 4 shows the accuracy obtained for both approaches. Through this comparison, it can be seen that the accuracy of HRTI exceeds 96% for all the given samples where the percentage is slightly higher compared to Gaussian.

Table 3. Area Error Percentage (AE%) of Gaussian and HRTI approach

Sample Location(s)	Gaussian AE(%)	HRTI AE(%)
1	3.36	1.11
2	4.35	2.20
3	1.13	0.61
4	4.16	2.91
5	6.10	2.25

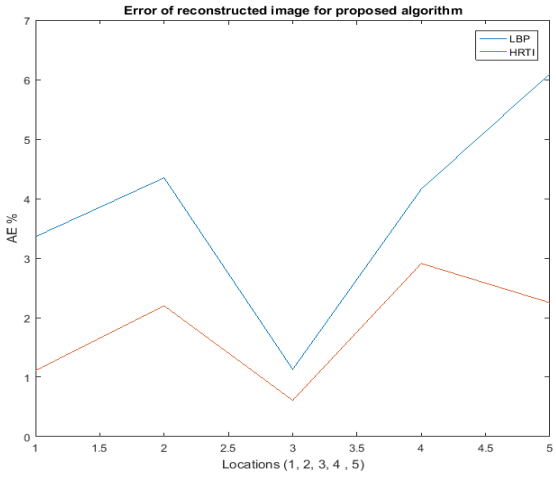

Figure. 9. Area error analysis graph

Table 4. Accuracy of localization projected by proposed algorithm

Sample Location(s)	Gaussian (%)	HRTI (%)
1	96.14	98.39
2	95.15	97.30
3	98.37	98.89
4	95.34	96.59
5	93.40	97.25

To concrete the finding, further analysis has been conducted using Structural Similarity Index Measure (MSSIM), Mean Squared Error (MSE) and Peak Signal to Noise Ratio (PSNR) to evaluate the performance of proposed method. All the result of performance analyses has been compiled in Table 3. Referring to the results, the performance of HRTI was much better compared to Gaussian for all the analyses performed. The reduction of the smeared area by HRTI helps to minimize the size of the peak area (which is our focus point in this study). Besides that, the SSIM analysis showed that a similarity result has been improved around 2% to 52% compared to the Gaussian. Which means the image constructed by HRTI is closer to the reference model. Meanwhile, the MSE analysis tested on the RTI image also shows HRTI performed well compared to Gaussian. Where, the MSE value recorded for HRTI and Gaussian are 552.9719 and 796.5407 respectively. The same goes for the PSNR evaluation for HRTI performance. It is seen to be slightly higher than Gaussian. Theoretically, known that the higher the PSNR, the better the quality of reconstructed image [8]. From all these analyses, known that HRTI performance is better and can be used to improve the quality of reconstructed images.

Table 4. Area Error Percentage (AE%), Structural Similarity Index Measure (SSIM), Mean Squared Error (MSE) and Peak Signal to Noise Ratio (PSNR)

Algorithm(s)	Gaussian			HRTI			Improvement (%)		
Sample(s)	MSSIM	MSE	PNSR	MSSIM	MSE	PNSR	MSSIM	MSE	PNSR
1	0.0333	650.0393	20.0014	0.0352	635.8968	20.0969	2.7737	1.0998	0.2382
2	0.0254.	711.9733	19.6062	0.0291.	655.4212	19.9656	6.7890	4.1358	0.9082
3	0.0184	796.5407	19.1187	0.0591	552.9719	20.7038	52.5161	18.0486	3.9804
4 (2 persons)	0.0061	1589.9355	16.1170	0.0217	986.0966	18.1916	56.1151	23.4407	6.0469
5 (2 persons)	0.0222	996.9417	18.1441	0.0270	938.1767	18.4080	9.7561	3.0368	0.7220

5. Conclusion

This paper presents HRTI as a new image reconstruction algorithm. Comparisons made between HRTI and Gaussian prove that HRTI performance is better. Where the accuracy of HRTI exceed 96%. However, tomographic images produced by HRTI still have the shadow area on the images which may affect the localization accuracy. Thus, future work will be focused on improving the quality image of HRTI and increase the accuracy of the localization.

Acknowledgment

The authors would like to thank the Ministry of Education Malaysia for their sponsorship and financial support. Appreciation and gratitude also for the Japan Science and Technology Agency, University of Yamanashi, and Center of Excellence for Advanced Sensor Technology (CEASTech), Universiti Malaysia Perlis for offering research collaboration opportunities under the Sakura Exchange Program in Science. Last but not least, many thanks to my supervisor and all postgraduate members under him for their help and support in this project.

References

[1] Wilson, J., Patwari, N., & Vasquez, F. G. (2009, June). Regularization methods for radio tomographic imaging. In *2009 Virginia Tech Symposium on Wireless Personal Communications*.

[2] Xu, S., Liu, H., Gao, F., & Wang, Z. (2019). Compressive sensing based radio tomographic imaging with spatial diversity. *Sensors*, *19*(3), 439.

[3] Wang, Q., Yiğitler, H., Jäntti, R., & Huang, X. (2015). Localizing multiple objects using radio tomographic imaging technology. *IEEE Transactions on Vehicular Technology*, *65*(5), 3641–3656.

[4] van der Meij, T. (2017). Mobile Radio Tomography: Agent-Based Imaging. In *BNAIC 2016: Artificial Intelligence: 28th Benelux Conference on Artificial Intelligence, Amsterdam, The Netherlands, November 10-11, 2016, Revised Selected Papers*, *765*, 63. Springer.

[5] Ortiz-Alemán, C., Martin, R., & Gamio, J. C. (2004). Reconstruction of permittivity images from capacitance tomography data by using very fast simulated annealing. *Measurement Science and Technology*, *15*(7), 1382.

[6] Xie, C. G., Huang, S. M., Lenn, C. P., Stott, A. L., & Beck, M. S. (1994). Experimental evaluation of capacitance tomographic flow imaging systems using physical models. *IEE Proceedings-Circuits, Devices and Systems*, *141*(5), 357–368.

[7] Rahiman, M. H. F., Rahim, R. A., Rahim, H. A., Muji, S. Z. M., & Mohamad, E. J. (2012). Ultrasonic tomography-image reconstruction algorithms. *International Journal of Innovative Computing, Information and Control*, *8*(1), 527–538.

[8] Hore, A., & Ziou, D. (2010, August). Image quality metrics: PSNR vs. SSIM. In *2010 20th international conference on pattern recognition*, 2366–2369. IEEE.